Evidence of Long-Term Correlation Between Clear-Air Attenuation and Scintillation in Microwave and Millimeter-Wave Satellite Links

Frank Silvio Marzano, *Member, IEEE*, and Carlo Riva, *Member, IEEE*

***Abstract*— Long-term correlation between microwave scintillation and path attenuation in clear-air troposphere is quantitatively evaluated carrying out a numerical and experimental analysis on a monthly basis. Amplitude scintillation variance is simulated by means of a weak-fluctuation propagation model, while path attenuation is obtained from ground-based brightness temperature data using a radiative transfer model. Both the scintillation and radiative transfer models are applied to a set of radiosounding observations, performed in Milan, Italy, during 1989. Regression formulas relating clear-air mean radiative temperature to meteorological quantities and slant-path attenuation to amplitude scintillation variance are derived from numerical simulations. Their validity should be restricted, in general, to mid-latitude subcontinental climates. Monthly predictions of radiometer-derived path attenuation and correlation between attenuation and scintillation are tested using both multichannel radiometric data and Italsat beacon measurements at 18.7, 39.6, and 49.5 GHz, acquired at Spino d'Adda, Italy, ground station in 1995. A fairly good agreement is found by performing a comparison between estimates and measurements.**

***Index Terms*— Clear-air amplitude scintillation, microwave propagation, satellite communications.**

I. Introduction

NEW fixed and mobile communication services are planned to exploit beacon frequencies at K band and above [1]. At these frequencies, scintillation plays an important role as a signal degradation source [2], [3]. Scintillation phenomena are attributed to turbulent refractive index inhomogeneity, which induces time and space random variations of the amplitude, the phase, and the angle of arrival of the received signal. The renewed interest in scintillation studies is mainly due to their relevant impact on digital links that have low fade margins available, but require high performance [4].

Recently, the application of electromagnetic propagation models, describing the interaction between microwave radiation and turbulent atmosphere, has been proposed for developing statistical prediction methods of clear-air scintillation using meteorological data [5]–[7]. This model-based approach has opened the possibility to include predictors other than surface data, showing that the vertically integrated water-vapor content is significantly correlated with the amplitude scintillation variance [6]. Indeed, this extension of the statistical prediction methods is very appealing since the integrated water-vapor content can be accurately retrieved by both dual-channel microwave radiometers [8], [9] and global positioning system (GPS) receivers [10], [11].

The foundations of these new estimation techniques are basically related to the correlation between clear-air scintillations and brightness temperatures. This correlation has been shown in literature by using both simulated and experimental data on a short- and long-term basis [6], [12]–[16]. Since path attenuation can be derived from radiometric measurements, it is expected that scintillation is also correlated with path attenuation in clear-air conditions, i.e., without clouds and precipitation.

An analysis of the correlation between rain path attenuation and scintillation intensity has been already carried out using Olympus measurements on a short-term basis [17]. In rain conditions, zenithal path attenuation at 20 GHz can reach values up to 15 dB (for precipitation intensity of about 50 mm/h). On the contrary, in clear-air conditions, we expect zenithal attenuation no greater than about 1 dB (for very humid air with 50 mm of vertically integrated water vapor) [18], [19]. This means that the dynamic range of path attenuation in clear-air conditions is much smaller than in rain conditions and, correspondingly, when clear-air high scintillation variances are present, the measured path attenuation values are generally small.

In this work, numerical and experimental evidence of the long-term correlation between microwave scintillation and path attenuation in clear-air troposphere is argued. Amplitude scintillation variance is derived both from a weak-fluctuation propagation model and from Italsat measurements at the Spino d'Adda ground station (Italy). Path attenuation is obtained from ground-based brightness temperature data, using both a radiative transfer model and a multichannel radiometric system available at the Italsat receiving station. Both the scintillation and radiative transfer models are applied to a set of radiosounding observations (RAOB's), performed in Milan, Italy, during 1989. Regression models, relating clear-air slant-path attenuation to amplitude scintillation, are derived from numerical simulations and tested against Italsat data.

Manuscript received January 22, 1999; revised October 5, 1999. This work was supported in part by the Italian Ministry of University and Scientific and Technological Research (MURST) and the Italian Space Agency (ASI).

F. S. Marzano is with the Dipartimento di Ingegneria Elettrica, Università dell'Aquila, Monteluco di Roio, L'Aquila, 67040 Italy.

C. Riva is with the Dipartimento di Elettronica e Informazione and Centro di Studio per le Telecomunicazioni Spaziali, Politecnico di Milano, Milano, 32-20133 Italy.

Publisher Item Identifier S 0018-926X(99)09974-3.

II. Theoretical Considerations

In this section, we will briefly introduce the basic relationships which relate, on the one hand, path attenuation to brightness temperature and atmospheric variables and, on the other hand, scintillation variance to the refractive-index structure constant and to atmospheric parameters. Within the outlined framework, the numerical and experimental analysis will be carried out in Sections III and IV, respectively.

Microwave tropospheric attenuation, during nonprecipitating conditions, is mainly caused by the spectral absorption of water vapor, oxygen, and cloud liquid water. Under the assumption of local thermodynamic equilibrium, the microwave thermal emission is expressed in terms of the equivalent blackbody brightness temperature (T_B) using the Rayleigh–Jeans approximation. Supposing a plane-parallel atmosphere and neglecting the scattering contribution (no rain conditions), the integral form of the radiative transfer equation allows one to express, explicitly, the brightness temperature as a function of the atmospheric parameters and optical thickness [8], [9].

The slant-path attenuation $A(f,\theta)$ [dB], calculated at a frequency f along an elevation angle θ (above the horizontal plane) at the altitude of a ground receiving station is related to the measured $T_B(f,\theta)$ as follows:

$$\begin{aligned}\langle A(f,\theta)\rangle &= \langle A(f,\theta=90^\circ)\rangle \operatorname{cosec}(\theta)\\ &= 4.343\langle \ln\left[(T_m(f,\theta)-T_c)/(T_m(f,\theta)\right.\\ &\quad \left.-T_B(f,\theta))\right]\rangle \end{aligned} \tag{1}$$

where the angle brackets indicate the long-term temporal averaging (in this work, on a monthly basis), T_m [K] is the mean radiative temperature and T_c [K] is the cosmic background brightness temperature (equal to 2.73 K), incident at the top of the atmosphere. The term $A(f,\theta=90^\circ)$ represents the zenithal attenuation and the cosecant law dependence is due to the assumption of a horizontally stratified atmosphere.

Note that due to the nonlinear form of (1), an explicit relationship between monthly $\langle A\rangle$ and $\langle T_B\rangle$ cannot be, in general, derived. However, if the ratio T_B/T_m is much less than one, (1) can be expanded into Taylor's series and a linear form can be used as a good approximation. The analysis of (1) reveals that the total attenuation can be estimated from microwave radiometric measurements, once T_m is known. It has been shown in the literature that T_m can be estimated from surface meteorological data, mainly from a combination of surface temperature T_s and relative humidity RH_s [8]–[9], [18]. However, we will show in the next section that the introduction of the vertically integrated water vapor V_c [mm or kg/m^2] can be also useful for accurately predicting T_m.

If the Taylor "frozen-in" hypothesis is assumed and the turbulent eddy sizes lie in the inertial subrange of the Kolmogorov spectrum, we can derive the following expression for the variance $\sigma_\chi^2(f,\theta)$ [dB^2] of plane-wave log-amplitude fluctuations χ [dB] at a frequency f due to horizontally stratified clear-air turbulence [5], [6], [14]

$$\begin{aligned}\sigma_\chi^2(f,\theta) &= 42.9G^2(\sin\theta)^{-11/6}k_o^{7/6}\\ &\quad\cdot\int_0^H F_s(z)C_n^2(z)z^{5/6}\,dz\end{aligned} \tag{2}$$

where G is the antenna-aperture averaging factor, θ is the elevation angle, k_o is the wave-number in vacuum, F_s is the intermittence factor due to atmospheric instability, C_n^2 is the refractive-index structure constant of homogeneous turbulence, and z is the altitude coordinate with H the effective height of turbulence [20]. Due to the log-normal probability distribution generally attributed to σ_χ^2, it is also common to refer to the scintillation log-variance $\ln(\sigma_\chi^2)$, conventionally expressed in Np.

Experimental and numerical analyses have shown that on a long-term basis the scintillation variance can be expressed as a function of the ground-based meteorological parameters. It is usual to adopt the following form for the long-term scintillation log-variance [6], [7], [21]

$$\langle \ln[\sigma_\chi^2(f,\theta)]\rangle = \ln[G^2 f^\alpha(\sin\theta)^{-\beta}] + \langle \ln[\sigma_{\chi n}^2(T_s,RH_s,V_c)]\rangle \tag{3}$$

where α and β are the frequency and angle scaling exponents, respectively, and $\sigma_{\chi n}^2$ is the normalized log-variance in general function of surface temperature T_s, relative humidity RH_s, and vertically integrated water vapor V_c in clear-air conditions. Comparing (2) with (3), we deduce that the theoretical values for α and β are 1.17 and 1.83.

If the refractive index is complex, as for the atmosphere in the microwave range where the absorption of water vapor (22–24 GHz) and oxygen (50–60 GHz) are dominant, (2) can be generalized [22]. In particular, it can be shown that the scintillation power due to absorption is mainly concentrated at low temporal frequencies and the high-pass cutoff frequency increases with the square root of the channel frequency. This means that, at K band and above, we would expect the bulk of the scintillation energy to be below 10 mHz [17].

In order to avoid this possible contamination in the correlation analysis, on the one hand, we have used an eighth-order Butterworth high-pass filter with a conservative cutoff frequency (at -3 dB) of 10 mHz [7]. On the other hand, we have decided to compute path attenuation from radiometric measurements using (1) instead of deriving it from beacon channel data. Actually, a frequency scaling should be applied for deriving the beacon path attenuation from the radiometric path attenuation on a long-term basis [18], [19].

III. Numerical Analysis

In order to simulate the observed T_B by a ground-based microwave radiometer at a given frequency and in a given direction, we have used the Liebe model to compute the atmospheric absorption [22]. This model gives a detailed description of the spectral molecular absorption of humid air (possibly with some cloud liquid) in the frequency range from 1 to 1000 GHz as a function of the local temperature, pressure, and relative humidity. The radiative transfer equation has been solved numerically considering a stratified atmosphere with levels associated to each RAOB level [8].

From the same stratified atmospheric model, we have also computed the scintillation variance through (2), discretizing the integral and using RAOB data (including the wind velocity) to evaluate both the intermittence factor F_s and the

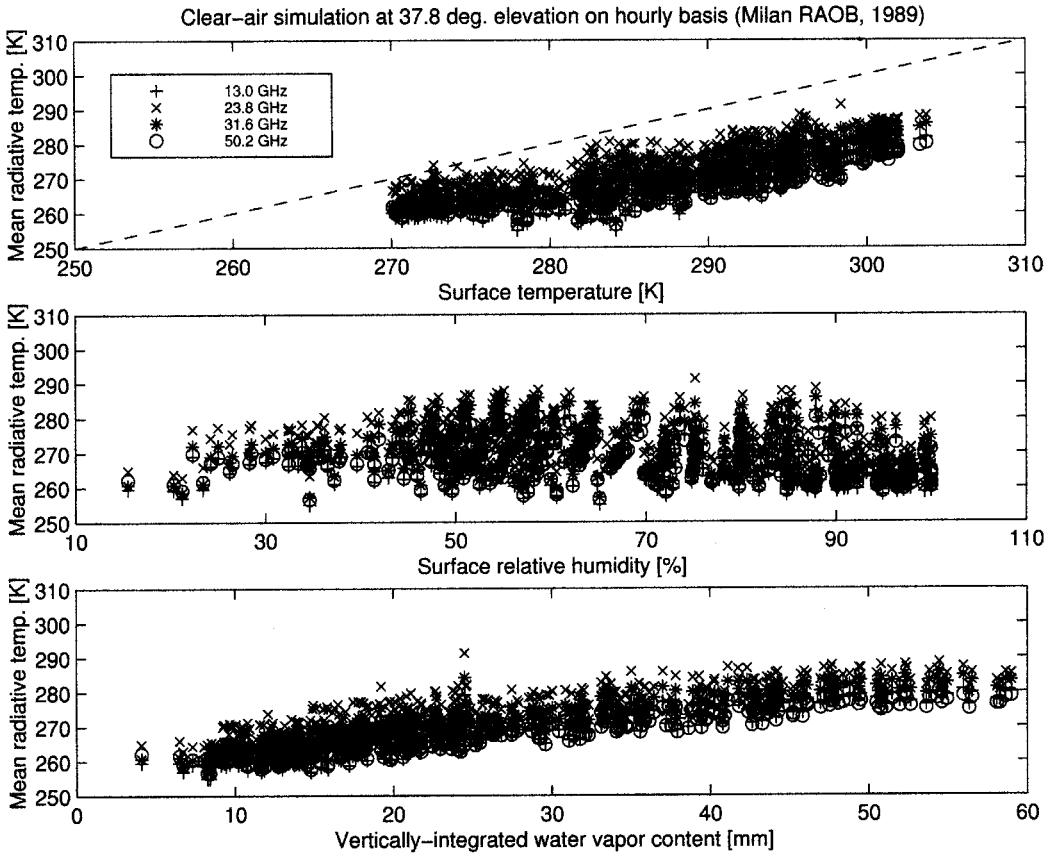

Fig. 1. Simulated mean radiative temperature at 13.0, 23.8 , 31.6, and 50.2 GHz against surface temperature, relative humidity and pressure on an hourly basis, using of clear-air RAOB data of 1989 (Milan, Italy) and an elevation angle of 37.8°. In the top panel the bisector is also indicated by a dashed line.

structure constant C_n^2 [6]. For the antenna aperture averaging factor G we have used the expression recommended by ITU-R [24]. To perform our simulations, we have selected clear-air RAOB's, acquired during 1989 twice a day around midday at 12:00 Greenwich Mean Time (GMT) and midnight at 24:00 GMT. It is worth mentioning that due to the time-zone and daylight saving time, GMT midday and midnight correspond to 2 PM and 2 AM local time from March to October and to 1 PM and 1 AM local time the rest of the year. Only clear-air RAOB's have been considered in this work, excluding the cloud presence by means of a humidity threshold [7], [9]. We have also considered beacon frequencies at 18.7, 39.6, and 49.5 GHz with a 37.8° elevation angle together with four radiometric frequencies at 13.0, 23.8, 31.6, and 50.2 GHz at the same 37.8° elevation angle. These simulation parameters are those of the Italsat ground station, later on considered in the experimental analysis.

Fig. 1 shows the simulated mean radiative temperature at 13.0, 23.8, 31.6, and 50.2 GHz against surface temperature, relative humidity and integrated water vapor content on an hourly basis (actually, only two hourly samples within a day), using clear-air RAOB data of 1989 (Milan, Italy) and supposing an elevation angle of 37.8°. In the top panel, the bisector is also indicated by a dashed line in order to show that the approximation $T_m = T_s$ is not generally adequate.

As expected, T_m at 23.8 GHz is higher than values at the other frequencies. Moreover, the fairly high correlation (0.81) between V_c and T_m is apparent from the bottom plot of the figure, meaning that the introduction of the vertically-integrated water vapor V_c can be also useful for accurately estimating T_m. In clear-air conditions, the following regression formula can be used to predict T_m on a short-term basis:

$$T_m(f,\theta) = a_0 + a_1 T_s + a_2 RH_s + a_3 V_c \qquad (4)$$

where the coefficients are function of the frequency, but are not strongly dependent on the elevation angle. In order to compute the coefficients of (4), we assumed an additive zero-mean Gaussian noise with a standard deviation of 1 K on T_s and 5% of the value on both RH_s and V_c. Table I provides these regression coefficients for each radiometric channel and in the 10–50 GHz band on an hourly basis, together with the root-mean square (rms) error. Note that inclusion of quadratic terms

TABLE I
COEFFICIENTS OF THE LINEAR REGRESSION (4) TO ESTIMATE SHORT-TERM MEAN RADIATIVE TEMPERATURE T_m [K] AT 13.0, 23.8, 31.6, AND 50.2 GHz AND IN THE BAND 13–50 GHz FROM SURFACE TEMPERATURE T_s [K], RELATIVE HUMIDITY RH_s [%], AND VERTICALLY INTEGRATED WATER VAPOR CONTENT V_c [mm], DERIVED USING RAOB DATA ACQUIRED IN MILAN, ITALY, DURING 1989, ASSUMING AN ELEVATION ANGLE OF 37.8°. ROOT-MEAN SQUARE ERROR IS ALSO INDICATED

Freq. [GHz]	a_0	a_1	a_2	a_3	*rmse [K]*
13.0	90.4692	0.5776	0.1147	0.1562	1.938
23.8	48.2414	0.7549	0.1421	0.0441	2.135
31.6	67.4157	0.6662	0.1289	0.1487	1.961
50.2	116.6953	0.4933	0.0975	0.1273	1.924
13.0-50.2	56.0999	0.7075	0.1412	0.0796	3.613

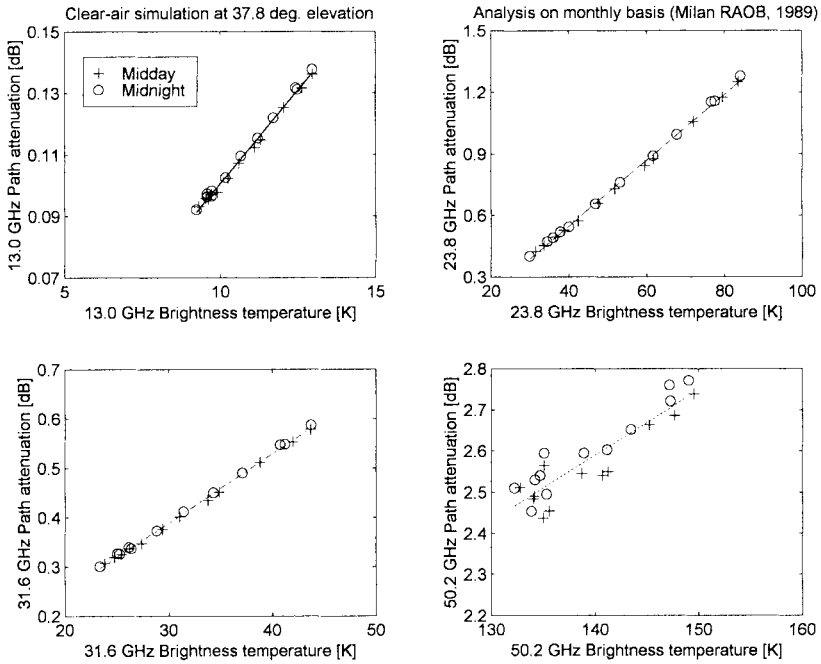

Fig. 2. Simulated brightness temperature and corresponding slant-path attenuation at 13.0, 23.8, 31.6, and 50.2 GHz on a monthly basis, using one year of clear-air RAOB data, Milan, Italy, 1989, at midnight and midday and supposing an elevation angle of 37.8°. Linear regression curves are also shown by dashed lines.

TABLE II
COEFFICIENTS OF THE LINEAR REGRESSION (5) BETWEEN LONG-TERM SLANT-PATH ATTENUATION $\langle A \rangle$ [dB] AND BRIGHTNESS TEMPERATURES $\langle T_B \rangle$ [K] AT 13.0, 23.8, 31.6, AND 50.2 GHz, DERIVED FROM THE SAME RAOB DATA SET OF TABLE I. THE ROOT-MEAN SQUARE ERROR AND CORRELATION COEFFICIENT ARE ALSO INDICATED

Freq. [GHz]	b_0	b_1	*rmse [dB]*	*correlation*
13.0	-0.0214	0.0122	0.001	0.997
23.8	-0.0895	0.0160	0.011	0.993
31.6	-0.0290	0.0140	0.004	0.999
50.2	0.3756	0.0158	0.041	0.909

in (4) does not modify substantially the estimation accuracy, while the introduction of V_c in (4), as a further predictor, gives improvements of about 10% in terms of rms error.

As anticipated, a linearized form of (1) can be derived in clear-air conditions. Fig. 2 shows the simulated slant-path attenuation at 13.0, 23.8, 31.6, and 50.2 GHz against the corresponding brightness temperature on a monthly basis, using the same data set as for Fig. 1 and supposing an elevation angle of 37.8°. In particular, for each month, both the midday and midnight values have been computed. The limited spread around the linear best-fit curves (only at 50.2 GHz the dispersion becomes significant) corroborates the assumption of a linear prediction formula; that is

$$\langle A(f,\theta) \rangle = b_0 + b_1 \langle T_B(f,\theta) \rangle. \tag{5}$$

Assuming an additive zero-mean Gaussian noise with a standard deviation of 1 K on T_B, Table II gives the coefficients of (5) to derive $\langle A \rangle$ from $\langle T_B \rangle$ at 13.0, 23.8, 31.6, and 50.2 GHz, together with the rms errors and the correlation coefficients.

After deriving long-term path attenuations from radiometric data through (5), we can statistically compare them with amplitude scintillation intensity statistics. Fig. 3 shows the simulated slant-path attenuation at 13.0, 23.8, 31.6, and 50.2 GHz against corresponding scintillation log variance at 18.7, 39.6, and 49.5 GHz on a monthly basis, using the clear-air RAOB data of Milan, Italy, 1989, and supposing an elevation angle of 37.8° and an antenna diameter of 3.5 m. Path attenuation at 23.8 GHz are higher than at 31.6 GHz due to the water-vapor peak absorption.

The latter figure justifies the assumption of a linear form to relate path attenuation and scintillation log-variance such as

$$\langle A(f,\theta) \rangle = c_0 + c_1 \langle \ln [\sigma_\chi^2(f,\theta)] \rangle \tag{6}$$

where the frequency f can indicate both a radiometric and a beacon channel, as shown later. In order to derive the regression coefficients of (6), given in Table III, we assumed an additive zero-mean Gaussian noise with a standard deviation of 1% of its value on $\ln [\sigma_\chi^2(f,\theta)]$. The rms errors and the correlation coefficients are also shown in the table. We have chosen to represent the scintillation log-variance, instead of its variance or standard deviation value, in agreement with the expression given in (3). Note that in order to get the variance value, it is not correct to take simply the exponential of the log-variance value due to the presence of the temporal average operator.

As expected, scintillation log-variances increase with frequency even though their dynamic ranges slightly decrease with frequency. This correlation between scintillation variances and path-attenuation basically depends on the solar heating of ground, which leads to an expected increase in the air temperature and absolute humidity, with a concomitant production of atmospheric instability and, thus, scintillation. Since brightness temperature represents the emitted thermal

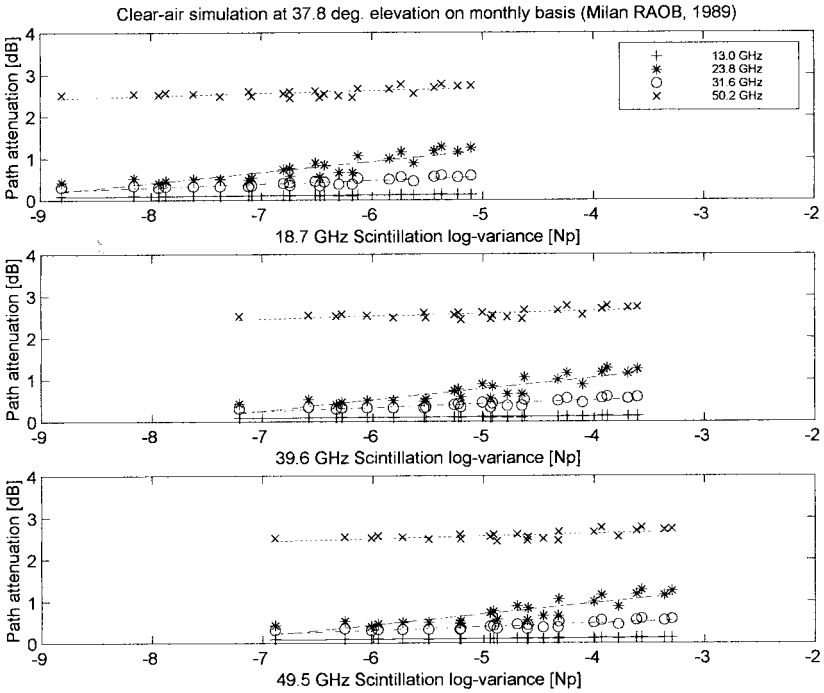

Fig. 3. Simulated slant-path attenuation at 13.0, 23.8, 31.6, and 50.2 GHz against corresponding scintillation log-variance at 18.7, 39.6, and 49.5 GHz on a monthly basis, using of clear-air RAOB data of Milan, Italy, 1989 and supposing an elevation angle of 37.8° and an antenna diameter of 3.5 m. Linear regression curves are also shown by dashed lines.

TABLE III
COEFFICIENTS OF THE LINEAR REGRESSION (6) BETWEEN LONG-TERM SLANT-PATH ATTENUATION $\langle A \rangle$ [dB] AT 13.0, 18.7, 23.8, 31.6, 39.6, 49.5, AND 50.2 GHz AND SCINTILLATION LOG VARIANCE $\langle \ln(\sigma_\chi^2) \rangle$ [Np] AT 18.7, 39.6, AND 49.5 GHz, DERIVED FROM THE SAME RAOB DATA SET OF TABLE I ASSUMING AN ELEVATION ANGLE OF 37.8° AND AN ANTENNA DIAMETER OF 3.5 m. THE rms ERROR AND CORRELATION COEFFICIENT ARE ALSO INDICATED

$\langle \ln(\sigma^2_\chi) \rangle$ at 18.7 GHz

Freq. [GHz]	*c0*	*c1*	*rmse [dB]*	*correlation*
13.0	0.1972	0.0132	0.008	0.852
18.7	0.8107	0.0816	0.043	0.879
23.8	2.4720	0.2581	0.138	0.879
31.6	0.9716	0.0841	0.047	0.868
50.2	2.9928	0.0626	0.078	0.619

$\langle \ln(\sigma^2_\chi) \rangle$ at 39.6 GHz

Freq. [GHz]	*c0*	*c1*	*rmse [dB]*	*correlation*
13.0	0.1787	0.0136	0.008	0.850
23.8	2.1094	0.2650	0.140	0.876
31.6	0.8537	0.0863	0.048	0.865
39.6	1.0681	0.0898	0.050	0.865
50.2	2.9056	0.0644	0.078	0.618

$\langle \ln(\sigma^2_\chi) \rangle$ at 49.5 GHz

Freq. [GHz]	*c0*	*c1*	*rmse [dB]*	*correlation*
13.0	0.1744	0.0136	0.008	0.848
23.8	2.0261	0.2651	0.141	0.874
31.6	0.8265	0.0864	0.048	0.863
49.5	2.4735	0.0680	0.083	0.616
50.2	2.8846	0.0643	0.079	0.616

radiation of the atmosphere, which, in turn, is due to atmospheric absorption, an increase in brightness temperature will be accompanied by an increase in observed path attenuation.

In order to scale radiometer-derived attenuation to beacon attenuation by using (5), we can carry out a further model investigation. Fig. 4 shows the simulated slant-path attenuation at 18.7, 39.6, and 49.5 GHz versus radiometer-derived slant-path attenuation at 13.0, 23.8, 31.6, and 50.2 GHz on a monthly basis, using of clear-air RAOB data of Milan, Italy, 1989, and supposing an elevation angle of 37.8°. Assuming a linear form and a single-variate dependence, it is possible to set the problem by means of the following regression formula:

$$\langle A(f_j, \theta) \rangle = d_0 + d_1 \langle A(f_i, \theta) \rangle \tag{7}$$

where the subscript j refers to the beacon channels and the subscript i refers to the radiometric channels under consideration. The regression coefficients needed to apply (7) for attenuation frequency scaling are given in Table IV, together with the rms errors and the correlation coefficients. Note that in (7) we have chosen to select the radiometric channel frequency f_i closest to the beacon attenuation frequency f_j. Multiple regression, using more than one predicting channel, can be also applied, but without significant improvements in the final accuracy.

TABLE IV
COEFFICIENTS OF THE LINEAR REGRESSION (7) BETWEEN LONG-TERM SLANT-PATH ATTENUATION $\langle A \rangle$ [dB] AT 18.7, 39.6, AND 49.5 GHz AND SLANT-PATH ATTENUATION $\langle A \rangle$ [dB] AT 13.0, 23.8, 31.6, AND 50.2 GHz, DERIVED FROM THE SAME RAOB DATA SET OF TABLE I. THE ROOT-MEAN SQUARE ERROR AND CORRELATION COEFFICIENT ARE ALSO INDICATED

Freq. [GHz]	*d0*	*d1*	*rmse [dB]*	*correlation*
18.7-23.8	0.0571	0.3161	0.001	0.999
39.6-31.6	0.2104	1.0405	0.002	0.999
49.5-50.2	-0.5547	1.0578	0.005	0.998

Scaling radiometer-derived attenuation to the Italsat beacon frequencies does not change the comments made for Fig. 3. This is shown in Fig. 5, where the scintillation log variances at 18.7, 39.5, and 49.5 GHz is plotted against the corresponding slant-path attenuation on a monthly basis. Table III reports the regression coefficients of (6) in this case, as well.

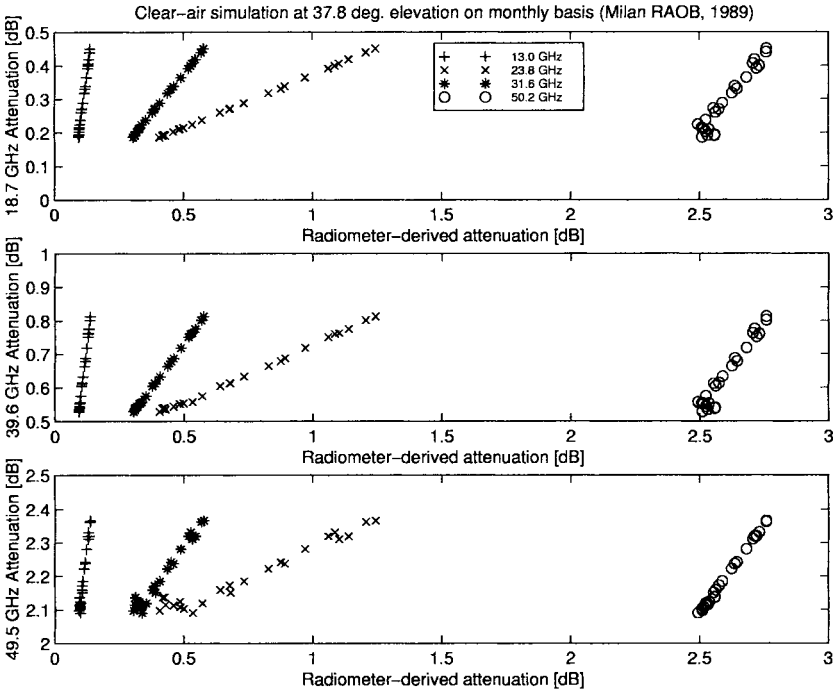

Fig. 4. Simulated slant-path attenuation at 18.7, 39.6, and 49.5 GHz versus radiometer-derived slant-path attenuation at 13.0, 23.8, 31.6, and 50.2 GHz on a monthly basis, using clear-air RAOB data of Milan, Italy, 1989, and supposing an elevation angle of 37.8°.

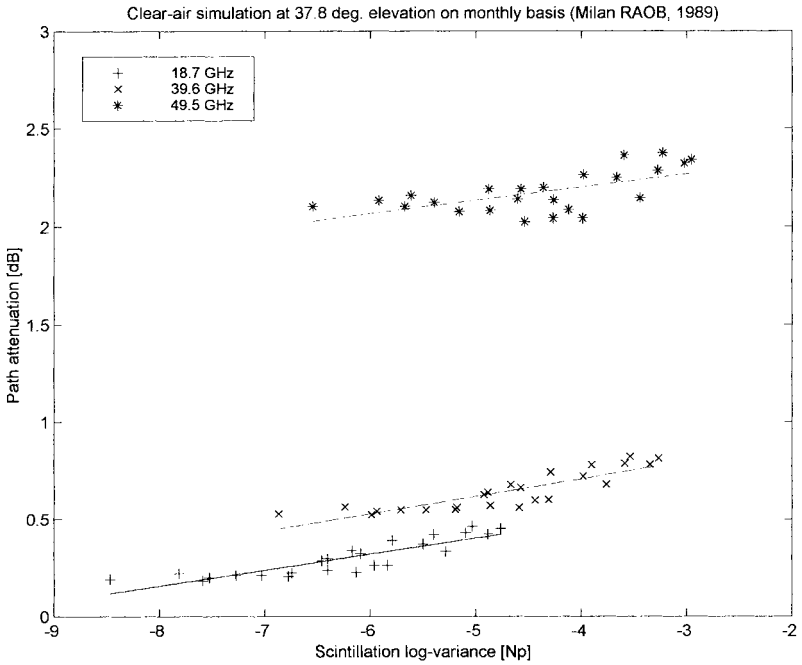

Fig. 5. Simulated and scintillation log-variance on a monthly basis, using of clear-air RAOB data of Milan, Italy, 1989, and supposing an elevation angle of 37.8° and an antenna diameter of 3.5 m. Linear regression curves are also shown by dashed lines.

IV. Experimental Analysis

We have considered measurements from the Italsat ground station in Spino d'Adda, Italy, close to Milan, where beacons at 18.7, 39.6, and 49.5 GHz are sampled at 1 Hz rate with antennas of 3.5-m diameter pointing at 37.8° elevation angle [4], [25]. A clear-sky threshold of −1.5 dB has been applied to the log-amplitude time series in order to select clear-air events, thus avoiding any deraining procedure [26]. High-pass filtered scintillation variances have been computed every minute [7]. Meteorological data, consisting of surface temperature and relative humidity, were measured at Spino d'Adda every ten minutes and four radiometric channels at 13.0, 23.8, 31.6, and 50.2 GHz pointing at 37.8° elevation angle as well, were also available at the same site. Radiometric systems were routinely

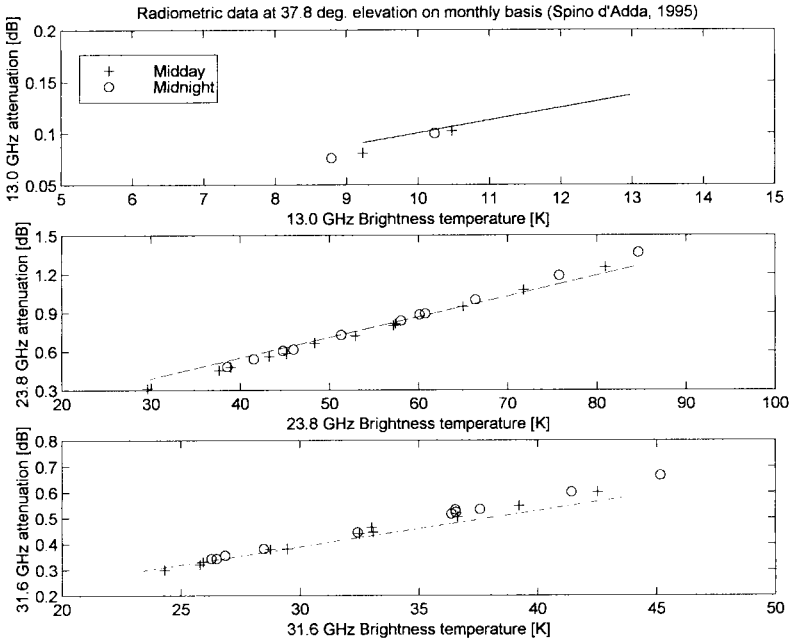

Fig. 6. Radiometer-derived slant-path attenuation against measured brightness temperature at 13.0, 23.8, and 31.6 GHz on a monthly basis, using clear-air radiometric data taken at the Italsat ground-station (Spino d'Adda, Italy) during 1995 at midnight and midday with an elevation angle of 37.8°. Linear regression curves, shown in Fig. 2, are also indicated for comparison.

calibrated by means of a tipping-curve method and they were used to cross check the presence of clouds and rain along the Italsat satellite path [8], [9].

For this work, twelve months of meteorological, radiometric, and beacon data have been available from January 1, 1995 to December 31, 1995 for the three beacons. Unfortunately, radiometric measurements at 50.2 GHz were not available continuously during the year so that it was not possible to include them in the experimental data set. Moreover, radiometric data at 13 GHz were considered reliable only in January and February.

Ground-station data time series were windowed around GMT midday and midnight (choosing a period of about 45 min) in order to make them consistent with the RAOB launch times used in the numerical analysis. Monthly averages of these windowed measurements were performed separately for midday and midnight data, thus providing 24 monthly mean values.

At Spino d'Adda, path attenuation for the Italsat beacon frequencies was derived by using a semi-empirical algorithm, not trained by the Milan RAOB data set as performed in this work [27]. Thus, a preliminary check of the prediction formula, as given in (5), can be a useful test to further apply (6). Fig. 6 shows the radiometer-derived slant-path attenuation against measured brightness temperature at 13.0, 23.8, and 31.6 GHz on a monthly basis, using one year of clear-air radiometric data taken at the Italsat ground-station (Spino d'Adda, Italy) during 1995 at midnight and midday with an elevation angle of 37.8°. Theoretical linear regression curves, as shown in Fig. 2, are also indicated for comparison. The agreement between the attenuation derived at Spino d'Adda and that obtained by using (5), is fairly good at 13.0 and 23.8 GHz (even though only four samples at 13 GHz were available). Some discrepancies are noted at 31.6 GHz, especially for path attenuation values greater than 0.5 dB, probably due to a calibration problem [27].

TABLE V
BIAS AND ROOT-MEAN SQUARE VALUE OF THE PERCENTAGE FRACTIONAL ERROR [%] DUE TO THE COMPARISON BETWEEN PATH ATTENUATION AT 13.0, 23.8, AND 31.6 GHz, DERIVED FROM RADIOMETRIC MEASUREMENTS, AND THAT ONE ESTIMATED FROM MEASURED SCINTILLATION LOG VARIANCE AT 18.7, 39.6, AND 49.5 GHz USING THE PREDICTION FORMULA (6)

Freq. [GHz]	*bias*	*rmse*	*Freq. [GHz]*	*bias*	*rmse*	*Freq. [GHz]*	*bias*	*rmse*
13.0-18.7	15.0	20.3	13.0-39.6	9.5	17.7	13.0-49.5	12.9	17.8
23.8-18.7	11.7	27.6	23.8-39.6	-0.9	30.4	23.8-49.5	12.2	38.2
31.6-18.7	2.6	22.2	31.6-39.6	-4.3	23.1	31.6-49.5	1.7	25.3

Finally, Fig. 7 shows the slant-path radiometer-derived attenuation at 13.0, 23.8, 31.6 GHz against the scintillation log variances at 18.7, 39.6, and 49.5 GHz on a monthly basis at midday and midnight. Theoretical linear regression curves, as shown in Fig. 3, are also indicated for comparison. Table V provides the quantitative results of this test in terms of the bias and rms value of the percentage fractional error, defined as the ratio between the attenuation $\langle A_m \rangle$, derived from radiometric measurements, minus the attenuation $\langle A \rangle$, predicted by (6), using beacon log-variances and the radiometer-derived attenuation itself; that is: $\varepsilon = 100\ (\langle A \rangle - \langle A_m \rangle)/\langle A_m \rangle$. The agreement between predicted and experimental data is fairly good, in particular at 18.7 GHz; the overall percentage rms error is less than 30%. The spread around the regression curves is higher at 23.8 GHz and the prediction algorithms seem to underestimate high-path attenuation corresponding to high-scintillation variance.

V. CONCLUSIONS

The long-term correlation between clear-air scintillation and slant-path attenuation has been analyzed using both synthetic

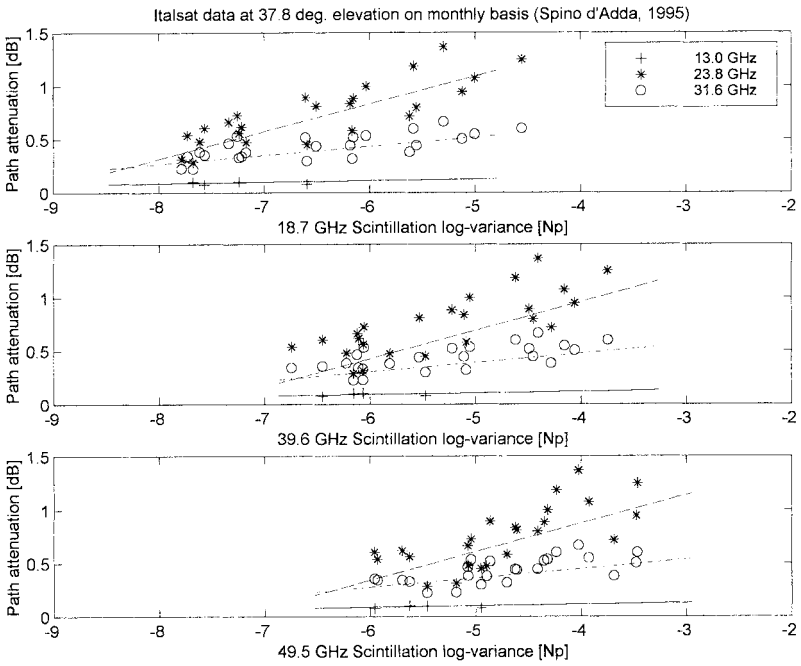

Fig. 7. Measured slant-path attenuation at 13.0, 23.8, and 31.6 GHz against scintillation log-variance at 18.7, 39.6, and 49.5 GHz on a monthly basis, using clear-air beacon and radiometric data taken at the Italsat ground-station (Spino d'Adda, Italy) during 1995 with an elevation angle of 37.8°. Linear regression curves, shown in Fig. 3, are also plotted for comparison.

and experimental data in the 20–50-GHz band. This statistical relationship has been derived quantitatively by using a coupled scintillation and radiative transfer model applied to RAOB data and has been tested against Italsat beacon data acquired in Spino d'Adda, Italy, during 1995. Slant-path attenuation has been derived from radiometric measurements, while scintillation variance has been evaluated by high-pass filtering the beacon time series. This choice has guaranteed the actual independence of the two data sources, thus avoiding the critical selection of the high-pass cutoff frequency.

Linear regression models have been extensively used to set up an effective procedure to retrieve path attenuation and scintillation log variance in clear-air conditions. Prediction formulas of short-term mean radiative temperature from meteorological measurement, long-term path attenuation from brightness temperatures, long-term path attenuation from scintillation log-variance, and beacon path attenuation from radiometric path attenuation, have been provided. It is worth mentioning that even though the results presented here are relevant to simulations at 37.8° elevation angle, by assuming (1) and (3) as a modeling framework, the angular dependence can be easily removed and the results generalized to observations with angles other than the one considered here.

This analysis can be summarized by concluding that on a monthly basis the clear-air beacon signal at K and V band has a scintillation log-variance, which is correlated with total path attenuation. This aspect could have some appealing impact in the link budget design and into the development of new scintillation prediction methods.

A possible weakness of the proposed approach is that only beacon data at GMT midnight and midday have been considered to coincide with available radiosonde data. The well-established diurnal pattern in scintillation intensity is generally peaked in the mid-afternoon so that the applicability of the model might fail for the prediction of the worst-case period of the day. However, as mentioned in Section III, GMT midday and midnight correspond to 2 PM and 2 AM local time for most year, thus taking into account the two possible extremes of scintillation activity. The adequateness of the selected data set has been also tested in [7] by evaluating the scintillation variance probability density functions derived from both simulation and Italsat data. A fairly good agreement with typical log-normal statistical distributions, widely reported in literature, was found. Nevertheless, a quantitative test of the developed methods against more complete beacon data sets will be pursued in the future. Further investigation should also include the evaluation of short- and long-term cloud effects on the correlation between path attenuation and scintillation variance

ACKNOWLEDGMENT

The authors would like to thank Servizio Meteorologico Aeronautica Militare Italiana, Rome, Italy, for kindly providing radiosounding data.

REFERENCES

[1] D. V. Rogers, L. J. Ippolito, Jr., and F. Davarian, "System requirements for Ka-band propagation effects on earth-satellite links," *Proc. IEEE*, vol. 85, pp. 810–821, June 1997.

[2] E. T. Salonen, J. K. Tervonen, and W. J. Vogel, "Scintillation effects on total fade distributions for earth-satellite links," *IEEE Trans Antennas Propagat.*, vol. 44, pp. 1–5, Jan. 1996.

[3] C. E. Mayer, B. E. Jaeger, R. K. Crane, and X. Wang, "Ka-band scintillations: Measurements and model predictions," *Proc. IEEE*, vol. 85, pp. 936–945, June 1997.

[4] B. R. Arbesser-Rastburg and A. Paraboni, "European research on Ka-band slant-path propagation," *Proc. IEEE*, vol. 85, pp. 843–852, June 1997.
[5] G. Peeters, F.S. Marzano, G. d'Auria, C. Riva, and D. Vanhoenacker-Janvier, "Evaluation of statistical models for clear-air scintillation prediction using Olympus satellite measurements," *Int. J. Satellite Commun.*, vol. 15, pp. 73–88, 1997.
[6] F. S. Marzano, and G. d'Auria, "Model-based prediction of amplitude scintillation variance due to clear-air tropospheric turbulence along earth-satellite microwave links," *IEEE Trans. Antennas Propagat.*, vol. 46, pp. 1–13, Oct. 1998.
[7] F. S. Marzano, C. Riva, A. Banich, and F. Clivio, "Assessment of model-based scintillation variance prediction on long-term basis using Italsat satellite measurements," *Int. J. Satellite Commun.*, vol. 17, pp. 17–36, 1999.
[8] E. R. Westwater, J. B. Snider, and M. J. Falls, "Ground-based radiometric observations of atmospheric emission and attenuation at 20.6, 31.65, and 90.0 GHz: A comparison of measurements and theory," *IEEE Trans. Antennas Propagat.*, vol. 38, pp. 1569–1580Oct. 1990.
[9] P. Ciotti, P. Basili, G. d'Auria, F. S. Marzano, and N. Pierdicca, "Microwave radiometry of the atmosphere: An experiment from a sea-based tower during the ERS-1 calibration," *Int. J. Remote Sensing*, vol. 5, pp. 133–148, 1995.
[10] M. Bevis, S. Businger, T. A. Herring, C. Rocken, R. A. Anthes, and R. H. Ware, "GPS Meteorology: Remote sensing of atmospheric water vapor using global positioning system," *J. Geophys. Res.*, vol. 97, pp. 15, 787-15, 801, 1992.
[11] O. T. Davies and P. A. Davies, "Comparison of integrated precipitable water vapor obtained by GPS and radiosondes," *Electron. Lett.*, vol. 34, pp. 645–646, 1998.
[12] A. Vander Vorst, D. Vanhoenacker, and L. Mercier, "Fluctuations on OTS-earth copolar link against diurnal and seasonal variation," *Electron. Lett.*, vol. 18, pp. 915–917, 1982.
[13] D. Vanhoenacker and A. Vander Vorst, "Experimental evidence of a correlation between scintillation and radiometry at centimeter and millimeter wavelenghts," *IEEE Trans. Antennas Propagat.*, vol. 33, pp. 40–47, Jan. 1985.
[14] J. Haddon and E. Vilar, "Scattering induced microwave scintillations from clear-air and rain on erath-space paths and the influence of antenna aperture," *IEEE Trans. Antennas Propagat.*, vol. AP-34, pp. 646–657, May 1986.
[15] P. Basili, G. d'Auria, P. Ciotti, P. Ferrazzoli, and D. Solimini, "Case study of intense scintillations along the OTS space-earth link," *IEEE Trans. Antennas Propagat.*, vol. 3, pp. 123–130, Jan. 1990.
[16] E. Matricciani, M. Mauri, and C. Riva, "Relationship between scintillation and rain attenuation at 19.77 GHz," *Radio Sci.*, vol. 31, pp. 273–279, 1996.
[17] B. Belloul, S. Saunders, and B. Evans, "Prediction of scintillation intensity from sky-noise temperature in earth-satellite links," *Electron. Lett.*, vol. 34, pp. 1023–1024, 1998.
[18] G. Schiavon, D. Solimini, and E. R. Westwater, "Performance analysis of a multifrequency radiometer for predicting atmospheric propagation parameters," *Radio Sci.*, vol. 10, pp. 631–650, 1993.
[19] F. Barbaliscia, E. Fionda, and P. G. Masullo, "Ground-based radiometer measurements of atmospheric brightness temperatures and water contents in Italy," *Radio Sci.*, vol. 33, pp. 697–706, 1998.
[20] G. d'Auria, F. S. Marzano, and U. Merlo, "Model of the refractive-index structure constant in intermittent clear-air turbulence," *Appl. Opt.*, vol. 32, pp. 2674–2680, 1993.
[21] Y. Karasawa, M. Yamada, and J. E. Allnutt, "A new prediction method for tropospheric scintillation on earth-space paths," *IEEE Trans. Antennas Propagat.*, vol. 36, pp. 1608–1614, Nov. 1988.
[22] R. H. Ott and M. C. Thompson, Jr., "Atmospheric amplitude spectra in an absorption region," *IEEE Trans. Antennas Propagat.*, vol. AP-26, pp. 329–332, Mar. 1978.
[23] H. Liebe, "An atmospheric millimeter-wave propagation model," *Int. J. Infrared Millimeter-Wave*, vol. 10, pp. 367–378, 1989.
[24] International Telecommunication Union-Radiopropagation (ITU-R), "Propagation data and prediction methods required for the design of earth-space telecommnucation systems," *Propagation in Non-Ionized Media*, Recommendation 618-6, Geneva, 1998.
[25] G. De Angelis, A. Paraboni, C. Riva, F. Zaccarini, G. Dellagiacoma, L. Ordano, R. Polonio, M. Mauri, and A. Pawlina, "Attenuation and scintillation statistics with Olympus and Italsat satellites in Italy," *Alta Frequenza*, vol. 6, pp. 66–69, 1994.
[26] S. M. R. Jones, I. A. Glover, P. A. Watson, and R. G. Howell, "Evidence for the presence of turbulent attenuation on low elevation angle earth-space links. Part 2—Frequency scaling of scintillation intensity on a 10 degree path," *IEEE Trans. Antennas Propagat.*, vol. 45, pp. 85–92, Jan. 1997.
[27] C. Capsoni, personal communication, Nov. 1998.

Frank Silvio Marzano (S'89–M'99) received the Laurea (electronic engineering) (*cum laude*) and the Ph.D. degrees (applied electromagnetics), both from the University "La Sapienza" of Rome, Italy, in 1988 and 1993, respectively.

In 1992, he was with a Visiting Scientist at Florida State University, Tallahassee, and in 1993, he collaborated with the Institute of Atmospheric Physics, CNR, Rome, Italy. From 1994 till 1996 he was with the Italian Space Agency and the Department of Electronic Engineering, University "La Sapienza," Rome, Italy, as a Postdoctoral Researcher. After being a lecturer in 1997, at the University of Perugia, Italy, he joined the Department of Electrical Engineering at the University of L'Aquila, Italy, where he is presently an Assistant Professor. His research mainly concerns passive and active remote sensing of the atmosphere from ground-based, airborne, and spaceborne platforms, radiative transfer modeling of scattering media, and tropospheric scintillation analysis along satellite microwave links.

Dr. Marzano received the Young Scientist Award of XXIV General Assembly of the International Union of Radio Science (URSI) in 1993. In 1998 he was the recipient of the Alan Berman Publication Award (ARPAD) from the Naval Research Laboratory, Washington, DC.

Carlo Riva (M'98) was born in Monza, Italy, in 1965. He received the Laurea degree (*cum laude*) in electronic engineering from the Politecnico di Milano, Italy, in 1990. From 1991 to 1994 he attended the Doctorate course in Electronic and Communication Engineering at the Politecnico di Milano in the propagation field with a special focus on scintillations.

In 1992, he was at European Space Research and Technology Centre, Noordwijk, The Netherlands, for three months, working on scintillation. In 1993 he was with the Universitè Catholique de Louvain, Louvain-la-Neuve, Belgium, for two months doing research on the separation of turbulence and rain effects on satellite communication links. He is currently with the Politecnico di Milano as an Assistant Professor with a research task in millimeter-wave propagation.